

1N-39
190806
30P

**NASA
Technical
Memorandum**

NASA TM - 108426

(NASA-TM-108426) AN ASSESSMENT OF
FINITE-ELEMENT MODELING TECHNIQUES
FOR THICK-SOLID/THIN-SHELL JOINTS
ANALYSIS (NASA) 30 p

N94-15534

Unclas

G3/39 0190806

**AN ASSESSMENT ON FINITE-ELEMENT MODELING
TECHNIQUES FOR THICK-SOLID/THIN-SHELL
JOINTS ANALYSIS**

By J.B. Min and S.G. Androlake

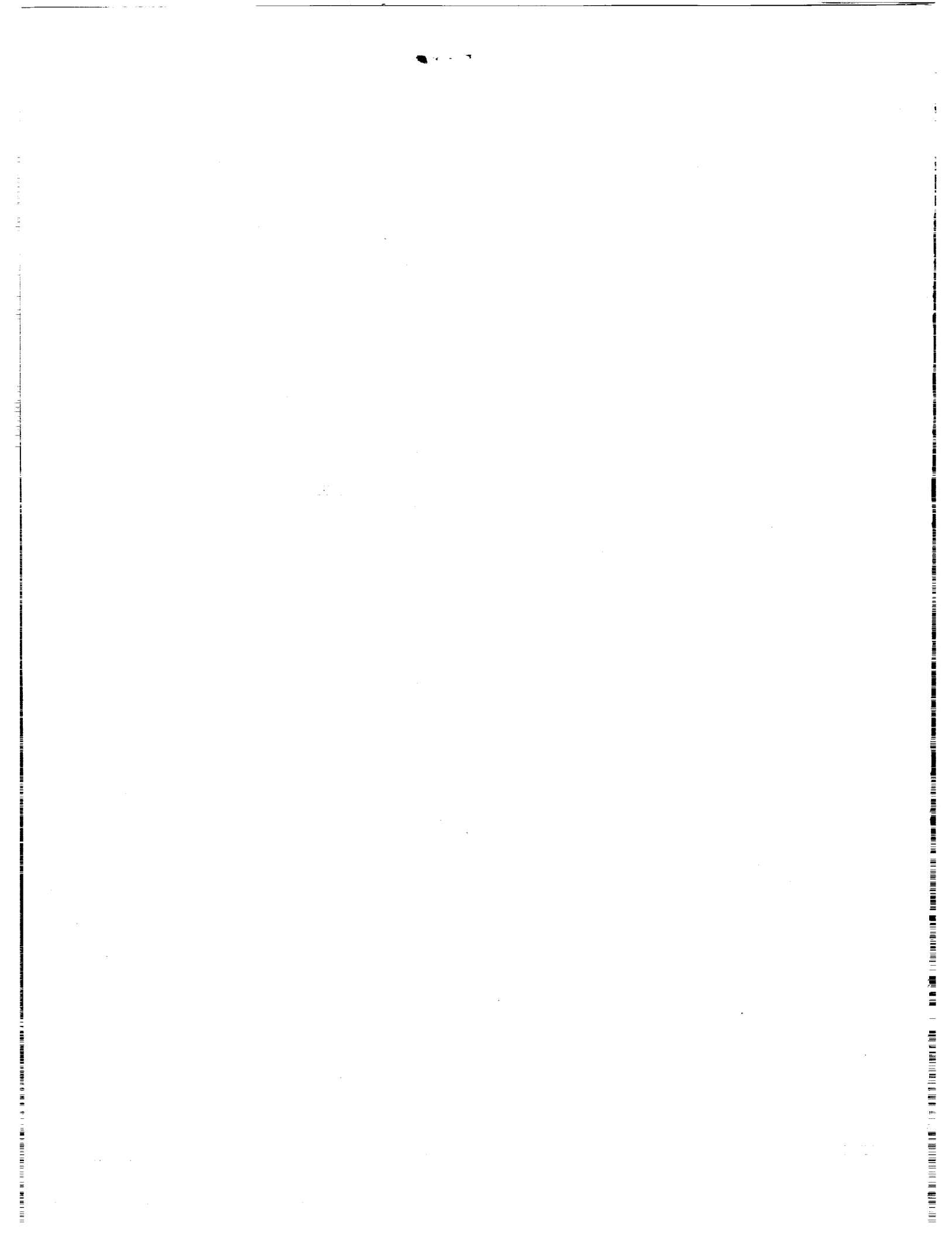
Structures and Dynamics Laboratory
Science and Engineering Directorate

October 1993



National Aeronautics and
Space Administration

George C. Marshall Space Flight Center



REPORT DOCUMENTATION PAGE

Form Approved
OMB No. 0704-0188

Public reporting burden for this collection of information is estimated to average 1 hour per response, including the time for reviewing instructions, searching existing data sources, gathering and maintaining the data needed, and completing and reviewing the collection of information. Send comments regarding this burden estimate or any other aspect of this collection of information, including suggestions for reducing this burden, to Washington Headquarters Services, Directorate for Information Operations and Reports, 1215 Jefferson Davis Highway, Suite 1204, Arlington, VA 22202-4302, and to the Office of Management and Budget, Paperwork Reduction Project (0704-0188), Washington, DC 20503.

| | | | | |
|---|---|--|---|--|
| 1. AGENCY USE ONLY (Leave blank) | | 2. REPORT DATE October 1993 | 3. REPORT TYPE AND DATES COVERED Technical Memorandum | |
| 4. TITLE AND SUBTITLE An Assessment on Finite-Element Modeling Techniques for Thick-Solid/Thin-Shell Joints Analysis | | | 5. FUNDING NUMBERS | |
| 6. AUTHOR(S) J.B. Min and S.F. Androlake | | | | |
| 7. PERFORMING ORGANIZATION NAME(S) AND ADDRESS(ES) George C. Marshall Space Flight Center Marshall Space Flight Center, Alabama 35812 | | | 8. PERFORMING ORGANIZATION REPORT NUMBER | |
| 9. SPONSORING/MONITORING AGENCY NAME(S) AND ADDRESS(ES) National Aeronautics and Space Administration Washington, DC 20546 | | | 10. SPONSORING/MONITORING AGENCY REPORT NUMBER NASA TM - 108426 | |
| 11. SUPPLEMENTARY NOTES Prepared by Structures and Dynamics Laboratory, Science and Engineering Directorate. | | | | |
| 12a. DISTRIBUTION/AVAILABILITY STATEMENT Unclassified—Unlimited | | | 12b. DISTRIBUTION CODE | |
| 13. ABSTRACT (Maximum 200 words) The subject of finite-element modeling has long been of critical importance to the practicing designer/analyst who is often faced with obtaining an accurate and cost-effective structural analysis of a particular design. Typically, these two goals are in conflict. The purpose of this study is to discuss the topic of finite-element modeling for solid/shell connections (joints) which are significant for the practicing modeler. Several approaches are currently in use, but frequently various assumptions restrict their use. In this study, such techniques currently used in practical applications have been tested, especially to see which technique is the most ideally suited for the computer-aided design (CAD) environment. Some basic thoughts regarding each technique are also discussed. As a consequence, some suggestions based on the results from this study are given to lead reliable results in geometrically complex joints where the deformation and stress behavior are complicated. | | | | |
| 14. SUBJECT TERMS Finite-element modeling techniques, solid/shell joints, computer-aided design (CAD), space shuttle main engine (SSME), stress singularity, global/local modeling, stress concentration factor, transition elements | | | 15. NUMBER OF PAGES 31 | |
| | | | 16. PRICE CODE NTIS | |
| 17. SECURITY CLASSIFICATION OF REPORT Unclassified | 18. SECURITY CLASSIFICATION OF THIS PAGE Unclassified | 19. SECURITY CLASSIFICATION OF ABSTRACT Unclassified | 20. LIMITATION OF ABSTRACT Unlimited | |

TABLE OF CONTENTS

| | Page |
|-----------------------------|------|
| INTRODUCTION..... | 1 |
| MODELS AND MATERIALS | 2 |
| RESULTS AND DISCUSSION..... | 4 |
| CONCLUSION..... | 6 |
| REFERENCES..... | 8 |

PRECEDING PAGE BLANK NOT FILMED

LIST OF ILLUSTRATIONS

| Figure | Title | Page |
|--------|--|------|
| 1. | Typical view of SSME..... | 9 |
| 2. | SSME high pressure fuel duct..... | 10 |
| 3. | Cylinder-to-cylinder intersection..... | 11 |
| 4. | (a) Shell model for a pipe tee, (b) local region of the model..... | 11 |
| 5. | 3-D solid model for a pipe tee..... | 12 |
| 6. | Combined shell and solid model for a pipe tee..... | 12 |
| 7. | Shell-to-shell intersection..... | 13 |
| 8. | Additional shell elements across the perpendicular free faces of solids..... | 13 |
| 9. | Model used for study (ref. 6)..... | 14 |
| 10. | Model A..... | 14 |
| 11. | Model B..... | 15 |
| 12. | Model C..... | 15 |
| 13. | Model D..... | 16 |
| 14. | Model E..... | 16 |
| 15. | Model F..... | 16 |
| 16. | Top view of model C..... | 17 |
| 17. | Top view of model D..... | 17 |
| 18. | Top view of model F..... | 18 |
| 19. | Front view of model C..... | 18 |
| 20. | Front view of model D..... | 19 |
| 21. | Front view of model F..... | 19 |
| 22. | Deflection U along length of model under horizontal load..... | 20 |

LIST OF ILLUSTRATIONS (Continued)

| Figure | Title | Page |
|--------|---|------|
| 23. | Deflection W along length of model under vertical load | 20 |
| 24. | Deflection W along $0 \leq x \leq 2.25$ under vertical load..... | 21 |
| 25. | Deflection U along $0 \leq x \leq 2.25$ under horizontal load | 21 |
| 26. | Deflection U along depth of model at $x = 2.0$ in under vertical load | 22 |
| 27. | Deflection U along depth of model at $x = 2.0$ in under horizontal load..... | 22 |
| 28. | Deflection U along depth of model at $x = 1.75$ in under vertical load | 23 |
| 29. | Deflection U along depth of model at $x = 1.75$ in under horizontal load..... | 23 |
| 30. | Deflection U along depth of model at $x = 1.5$ in under vertical load | 24 |
| 31. | Deflection U along depth of model at $x = 1.5$ in under horizontal load..... | 24 |



TECHNICAL MEMORANDUM

AN ASSESSMENT ON FINITE-ELEMENT MODELING TECHNIQUES FOR THICK-SOLID/THIN-SHELL JOINTS ANALYSIS

INTRODUCTION

In many industrial applications, there are three-dimensional (3-D) solid continua with thin shell-like portions connected to them such as duct flange joints, turbine blades mounted on a shaft, and shell intersections and branches, as can be seen in the space shuttle main engine (SSME) (figs. 1 and 2). In general, for finite-element modeling of such structures, the 3-D solid elements as well as thin-shell elements are employed. The analysis capabilities for the plates, shells, and thick solid structures have been considerably enhanced with the advances in the curved solid and shell finite elements.^{1 2} The general-purpose finite-element computer programs,^{3 4} which have implemented these finite elements, led to their use in the day-to-day design and analysis processes.

However, the modeling of the connections (joints) of shell elements to the solid elements presents considerable difficulty, since the nodal degrees-of-freedom (DOF) for these types of elements are incompatible with each other. Attempts to discretize shell-like portions of the structure with solid elements are not only time consuming and impractical, but may also lead to erroneous results for thin-shell structures. Therefore, suitable modeling of the connection regions where the solids connect to the shells is of considerable interest to the modelers, because often these regions are the weakest regions, and their accurate modeling is necessary for determining correct stresses and deformations.

For instance, when analyzing welded connections such as tubular joints (fig. 2),⁵ intersecting shells may require solid elements to adequately consider the 3-D stress state and weld geometry at the shell junctions. However, the use of solid elements for the thin portions of the model is uneconomical because the need for a reasonable aspect ratio would require an unnecessarily fine mesh. In addition, curved solid elements introduce extra DOF's in situations for which shell elements are adequate. Therefore, there is a need for an element that is capable of connecting curved shell elements to solid elements.

Such elements have been reported for linear⁶ and geometrically nonlinear analysis.⁷ These elements use reduced integration to avoid the well-known transverse shear and membrane locking phenomenon. However, without modification, these elements are unacceptable for general purpose finite-element codes because the use of reduced integration often leads to the existence of spurious zero energy modes or mechanisms. Therefore, an accurate shell/solid transition element that does not require reduced integration is desirable for both general linear and nonlinear analysis. Recently, Bathe and Dvorkin⁸ and Huang and Hinton⁹ recognized that, though locking in shell elements results from artificial strain energy terms that exist at all points within the element except at reduced integration sampling points, the actual use of reduced integration leads to spurious mechanisms. The solution was to use full numerical integration. However, rather than defining strain components directly from nodal displacements at each integration point, the nodal displacements were obtained by interpolating (or extrapolating) them from the points at which they are known to be accurately represented. Also, a similar approach was used by Cofer and Will.¹⁰ Although these solid/shell

transition elements were reported in the references mentioned above, they are not implemented in the currently available commercial codes. Some other approaches for a practical purpose are currently in use. However, frequently various assumptions restrict their use. Therefore, an assessment of such approaches has been attempted in this study through the tests so as to give an idea of which analysis technique can be ideally suited for solid/shell joint problems, particularly in the computer-aided-design (CAD) environment.

In the next sections, basic thoughts regarding each technique will be discussed, and they will be concluded with some suggestions based on the results obtained.

MODELS AND MATERIALS

Each technique was tested to evaluate its performance and compared to the results given in the reference.⁶ Prior to presenting the models considered in this study, it is appropriate to explain the problems which occur in solid/shell joint modeling.

As a first example, a simple pipe tee¹ (fig. 3) will be taken. The geometry is prescribed, and the loading and support locations are indicated. However, there are many different finite-element models that could be used for just a simple linear static analysis. The joint could be modeled by using connecting beam elements, connecting straight pipe elements, or a specialty element for pipe tee joints. However, if a detailed stress distribution is required at the branch to main-run junction, a totally different model must be used. One detailed model, for example, may use all shell elements (fig. 4); a second model may use all solid elements (fig. 5); a third possibility is a mixture of solids and shell elements (fig. 6). Each of these models has a different theoretical basis and potential cost. The "best" model is the one that accurately answers the questions involved with a minimum of time and cost.

The most common approach for thin-shell structures uses plate and/or shell elements throughout the model. The shell model properly represents the loads and deflections throughout, with the shell elements simulating the shell theory response well. However, in the region of the intersection of the shells (fig. 7), there is potential for relatively high error in the stress calculations. First, the thin-shell model connects only the midsurface planes of the elements. Figure 7 shows the poor representation of shell junctions with midsurface connections. It is just assumed that the nodal deflections and nodal forces are compatible along the edges. Second, the flat-plate or shell elements of commercial codes have a different order of displacements for membrane and bending actions. The membrane (in-plane) displacement functions are linear, bilinear, or incomplete quadratic, while the bending (lateral) displacements are usually cubic or incomplete quadratic. When two such elements are connected, the displacements (hence, forces and stresses) can be highly incompatible along the edge boundaries. This happens when the elements do not lie in the same plane. Although the coordinate transformations are utilized to avoid this incompatibility, the plate and/or shell models are not completely satisfactory for intersecting shell structures, but are good if the stresses at the line of intersection are not important. However, if complete stress patterns, including concentrations, may be required, the system requires a full 3-D model (fig. 5) or a combined shell and solid model (fig. 6). A mixture of solid and shell elements has been employed for the SSME structural analyses.

The combination of shell and solid elements requires special modeling techniques. Shells have six DOF per node—three translations and three rotations. Solids have only three DOF—all

translations. Special linear-constraints equations may be imposed on the common nodes to couple rotation of the shell to differential translation of the solid. As mentioned earlier, in complex junctions where deformation and stress behavior are complicated, such an approximation may lead to unreliable results.

Another technique for combining DOF involves the use of additional shell elements across the perpendicular free faces of the solids (fig. 8). These shell elements share the same nodes with the solids and must be very stiff in bending and flexible in membrane to connect to the solids. Thus, special constraint equations have to be imposed to handle this requirement.

The subject of suitable finite-element modeling for solid/shell connections is very important to the practicing analysts faced with obtaining accurate results.

With this background for the problem, a cantilever plate, used in reference 6 and shown in figure 9, was taken in this study to understand the modeling techniques used practically for solving these joint problems. However, stress calculation was not attempted to assess the performance of the techniques because of the unavailability of reference data to be compared to the stress results obtained. In all the cases considered in this study, only the deflection details are provided.

The plate consists of a short, thick metal slab (2 by 1 by 0.7 in) and a very thin long plate (10 by 1 by 0.1 in) jointed together at the middle plane ($z = 0.35$ in). The plate is subjected to a bending load of 3 lb/in (loading I) and an in-plane load of 12×10^4 lb/in (loading II) at the free end of the plate ($x = 12$ in), respectively. The plate material has a Young's modulus of 30×10^6 lb/in² and a Poisson's ratio of zero. The ANSYS code³ was used for models. Details of the finite-element models considered in this study are given as the following.

Model A:

Figure 10 shows a finite-element model used 20 8-node solid elements and 28 4-node shell elements. Solid elements and shell elements joined together at $x = 2$ in, without writing any constraint equations.

Model B:

The 1.95- by 1- by 0.7-inch portion of the plate is modeled with 20 8-node solid elements. The 10- by 1- by 0.1-inch portion was modeled with 28 4-node shell elements. The 0.1- by 1- by 0.1-inch beam elements were used between solid elements and shell elements without writing any constraint equations. The details of the model are shown in figure 11.

Model C:

The 2- by 1- by 0.6-inch portion of the plate was modeled with 8 20-node solid elements and also with 2 8-node shell elements. The 12- by 1- by 0.1-inch portion of the plate was modeled with seven eight-node shell elements at $z = 0.35$ in. Model C is illustrated in figure 12.

Model D:

The entire structure was modeled using 17 20-node solid elements. Model D is illustrated in figure 13.

Model E:

The 1.9- by 1- by 0.7-inch portion of the plate was modeled with 20 8-node elements. The 0.1- by 1- by 0.7-inch portion of the plate was modeled with 10 4-node shell elements which were attached to the solid, and then 28 4-node shell elements for the 10- by 1- by 0.1-inch portion of the plate were used. Model E is illustrated in figure 14.

Model F:

The entire plate was modeled using eight-node shell elements. The 2- by 1- by 0.7-inch portion was modeled with two eight-node shell element (element thickness 0.7 inch), whereas the remainder of the plate was modeled using seven eight-node shell elements (element thickness = 0.1 in). Model F is illustrated in figure 15.

RESULTS AND DISCUSSIONS

The results of test cases are presented in this section. Only the deflections are compared with those given in reference 6 for both loading cases shown in figure 9.

The analyses for the models A, B, and E were terminated due to the negative equation solver pivot terms. To give a better understanding of this error, it is appropriate to describe the Gauss elimination solution of equations (or wave-front equation solver). Using standard abbreviations, the stiffness equation is $\{K\} [D] = \{R\}$, where $\{K\}$ is the stiffness matrix, $[D]$ is the displacement vector, and $\{R\}$ is the load vector. The first equation is symbolically solved for D_1 , then substituted into the subsequent equations. The second equation is similarly treated, then the third, and so on. This forward-reduction process alters $\{R\}$ and changes $\{K\}$ to upper triangular form, with 1's on the diagonal. Finally, unknowns are found by back-substitution, so that the numerical value of D_1 is found last. This simple approach is acceptable because pivot terms are not small unless the structure is nearly unstable or badly modeled. A warning message can be printed if pivot terms are uncomfortably small, and execution can be terminated if pivot terms are unacceptably small. If pivot terms are negative, the structure is unstable.²

In order to prevent the analysis termination due to negative equation solver pivot terms in models A, B, and E, constraint equations may be used to relate the displacements of selected nodal points between the dissimilar elements. However, such approximations may lead to unreliable results as mentioned above. Therefore, the finite-element modeling techniques that have been considered for solid-shell connections using the techniques of models A, B, and E would not be practical.

No constraint equations were imposed on the models in this study. Thus, comparisons were made only with the results from models C, D, and F and with those given in reference 6. The deformed shapes on the undeformed shapes of models C, D, and F are shown in figures 16 to 18 for horizontal loads and in figures 19 to 21 for vertical loads, respectively.

Figure 22 shows a plot of the deflections in the x -direction along the length of the plate for each model under horizontal (in-plane) load. A plot of the deflections in the z -direction along the

length of the plate under vertical (out-of-plane) load is shown in figure 23. As can be seen, models C, D, and F show quite good agreement with the results given in reference 6.

Figures 24 and 25 show the deflections in the z -direction under vertical load and the deflections in the x -direction under horizontal load along the plate length from $x = 0.0$ inch to $x = 2.25$ inches. The purpose of this plot was to show the sharp change in deflection from $x = 2.0$ inches to $x = 2.25$ inches. This was expected since the selection at $x = 2.0$ inches has stress singularity due to sudden change in thickness. In figure 24, it was observed that though the result from model C is close to the results from the other cases, models D and F indicate better agreement with the values given in reference 6. However, it was indicated in figure 25 that models C and D yield better agreement with the values given in reference 6.

Figures 26 and 27, 28 and 29, and 30 and 31 show the deflections in the x -direction along the depth of the beam at $x = 2.0$ inches, $x = 1.75$ inches, and $x = 1.5$ inches for each model under vertical and horizontal loads, respectively. As shown, model F failed to capture the correct deflections because it was a plate model. In figure 26, model C showed quite different results from those of model D and reference 6. This figure also indicates that model D does not show good agreement along the depth of the beam at $0.2 \text{ inch} < z < 0.35 \text{ inch}$ with the values given in reference 6. One possibility for this discrepancy could be due to the coarseness of model D mesh or the poorly defined transition element used in reference 6. Also, as observed in figure 27 for the horizontal loading cases, it was shown that the results from model C and D did not correlate well with those given by reference 6. In figures 28 and 29 at $x = 1.75$ inches and figures 30 and 31 at $x = 1.5$ inches, similar responses were indicated as those observed at $x = 2.0$ in shown in figures 26 and 27. However, at the locations away from the region of stress singularity ($x = 2.0$ inches) the increasing correlation in the results can be observed. An interesting point was also observed in figure 31 showing that the result given in reference 6 shows quite different results when compared to those from models C and D. Consequently, although model C might be an acceptable technique to predict the deflections in a practical sense, care must be given in using the technique of model C. Furthermore, the important thing to be mentioned here is that though model C displays practically predictive capability in deflections, the variations of stresses and strains are of higher order than displacements within the elements. Therefore, a model which gives a good displacement solution may not give a good solution in stress.

In general, the constant-stress element is the most basic element and satisfies the basic convergence criteria for elements. As a mesh is refined, the solution converges, but because stress in each element is constant, equilibrium cannot be satisfied between elements except in regions where stress does not actually vary. Therefore, for problems with high-stress gradients, an exceptionally fine mesh is required for an accurate solution. Also, elements with quadratic and higher-order stress fields require cubic or higher-order displacement functions, and they have either more nodes per element or more DOF per node, which makes them inherently more expensive elements. Besides, complex structures require relatively fine meshes to model the geometry and stress discontinuity properly. As a result of the limitations in the modeling techniques described above, alternate approaches would be desired.

A global/local modeling approach, with relatively coarse global-response models and detailed local models, could be considered. The global model ensures that the load path simulates overall response and provides adequate stress results away from the discontinuity. A local model, on the other hand, provides detailed maximum stresses in the region of discontinuities.

There are two basic methods for detailed local modeling of stresses near regions with discontinuity. The first involves using a refined mesh so that the peak stresses at the discontinuity can be computed. This entails several transitions of analyses, thereby complicating the total analysis. Usually the mesh must be refined several times near the discontinuity to prove convergence of the solutions, a process which can be expensive and time-consuming. The second method¹⁰ models the structure for an accurate primary stress pattern immediately outside the region of discontinuity. In the computation of the maximum-stress state, the stress-concentration factor K_t should be applied to the primary stress. The primary stress value should include all gross structural effects, but should not include any local effects from the discontinuity. Thus, the choice is between creating a refined mesh at the discontinuity or applying a stress concentration factor to stresses from a linearized solution in order to obtain the good predictive stresses in the problems with high-stress gradients.

CONCLUSION

An important and large application area for shell/solid analysis will be the CAD environment. In this area, linear and nonlinear shell/solid analysis will be conducted in routine applications using the CAD system. Therefore, the analysis capabilities must be versatile, robust and above all things for all possible analysis conditions.

In this study, some practical finite-element modeling techniques currently used for the thick-solid/thin-shell connections analysis, especially using the CAD systems, have been tested in order to determine which technique is the most ideally suited for CAD environments. As a result of this study, two basic approaches are suggested for determining correct stresses and deformations of the thick-solid/thin-shell joint problems.

The first technique is to use global/local modeling. Local modeling involves the evaluation of the system using a model which provides the correct total response and a correct representation of stresses away from any discontinuities. Therefore, the global models can be relatively coarse, and total-response analysis is cost-effective. Only the local regions have refined meshes, and these models include only displacement boundary effects computed from the total response. The global analysis would use the shell elements, while the local model would use only the 3-D solid elements. The shell displacement field is imposed on the solid-model boundaries. As in other special techniques, this local model should be created sufficiently away from the region of interest for stress. Local modeling can then be used for the local stress calculations. This method also needs special techniques (i.e., interpolation or extrapolation techniques) for the interfaces between the global model and the local model, as is usually required in order to satisfy compatibility.

The second technique is to develop transition elements which are currently not available in the commercial codes. In the analysis of an actual shell structure, it is desirable to model shell intersections and shell-to-solid transitions effectively (without writing unreliable constraint equations) using transition elements. However, in development of the transition elements, the following requirements should be satisfied to render the elements widely applicable in routine applications using the CAD system:

- (1) The element should be applicable to any solid/shell situation.
- (2) The element should not contain any spurious zero energy modes.

- (3) The element should be simple and inexpensive to use with any solid/shell elements.
- (4) The element should be insensitive to element distortions.
- (5) Any restrictions/fictitious conditions should not be imposed.
- (6) The element can be used for thin to thick shell structures.
- (7) The element should be used for either material or geometrical nonlinearities.
- (8) Since transition elements are a connecting link between solids and shells, the stress and strain characteristics of these elements should be such that as we move from the solid element face toward the shell element face, the stresses and strains should also make a transition from those like solids to those like shells.

REFERENCES

1. Zienkiewicz, O.C.: "The Finite Element Method in Engineering Science." McGraw-Hill, London, United Kingdom, 1985.
2. Cook, R.D.: "Concepts and Applications of Finite Element Analysis." Wiley, New York, NY, 1981.
3. DeSalvo, G.J., and Swanson, J.A.: "ANSYS User's Manuals." Swanson Analysis System, Houston, PA, 1991.
4. Hallquist, J.O.: "DYNA Codes and NIKE Codes User's Manuals." Lawrence Livermore National Laboratory, Livermore, CA, 1988.
5. SSME Structural Audit: SSME HPFD 4.2 Bleed Valve Connection, Rocketdyne Division, Rockwell International, 1992.
6. Surana, K.S.: "Transition Finite Elements for Three-Dimensional Stress Analysis." Int. J. Numer. Meth. Engng. 15, 1980, pp. 991-1020.
7. Surana, K.S.: "Geometrically Nonlinear Analysis." Computers and Structures, vol.15, No.5, 1982, pp. 549-566.
8. Bathe, K.J., and Dvorkin, E.N.: "A Formulation of General Shell Elements—The Use of Mixed Interpolation of Torsorial Components." Int. J. Numer. Meth. Engng. 22, 1986, pp. 697-722.
9. Huang, H.C., and Hinton, E.: "A New Nine Node Degenerated Shell Element With Enhanced Membrane and Shear Interpolation." Int. J. Numer. Meth. Engng. 22, 1986, pp. 73-92.
10. Cofer, W.F., and Will, K.M.: "A Three-Dimensional, Shell-Solid Transition Element for General Nonlinear Analysis." Computer and Structures, vol. 18, No. 4, 1991, pp. 449-462.
11. Kelly, F.S.: "Mesh Requirements for the Analysis of Stress Concentration by the Specified Boundary Displacement Method." Proc. Second Int. Comput. Eng. Conf., ASME, New York, NY, August 1982.

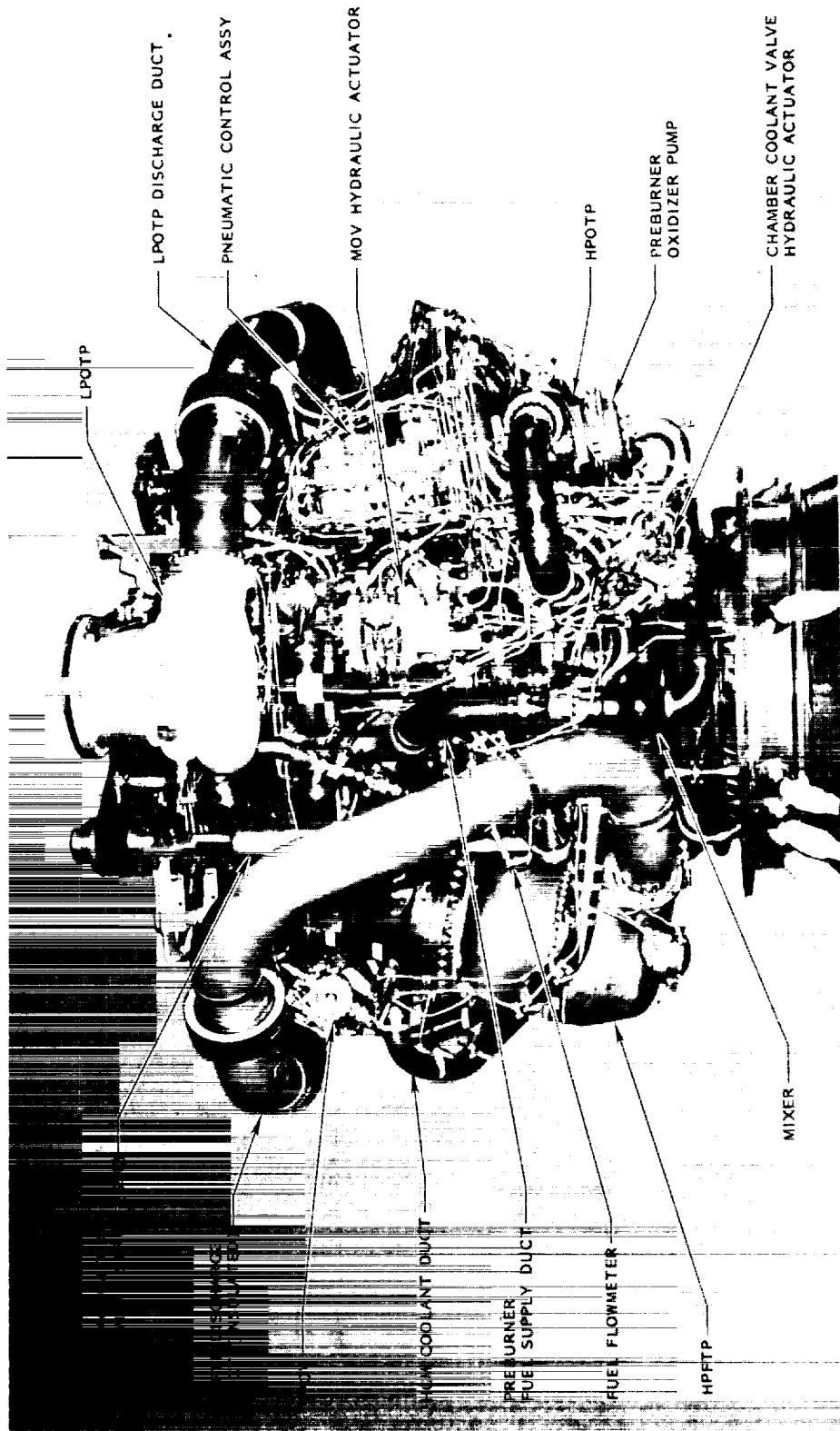


Figure 1. Typical view of SSME.

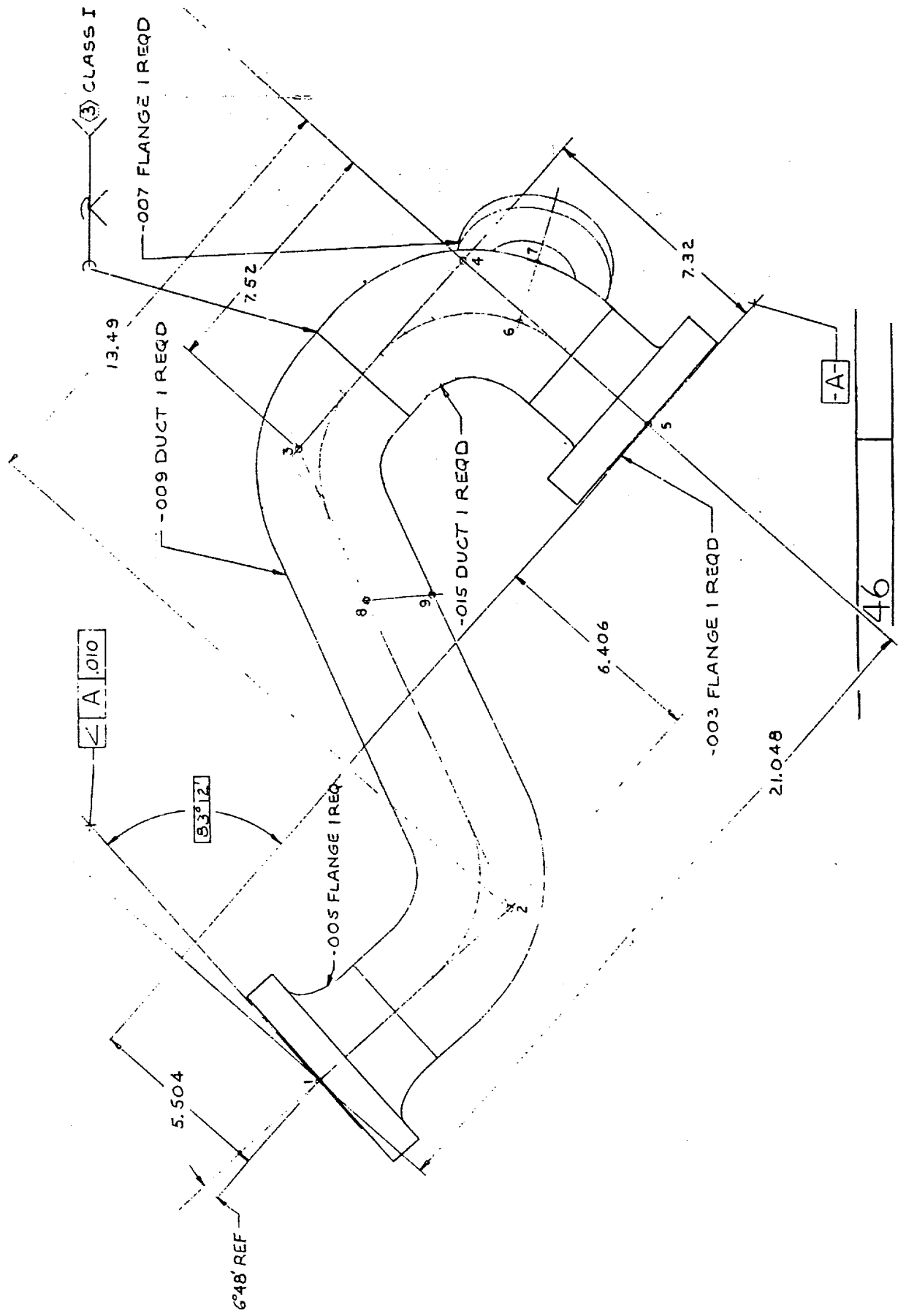


Figure 2. SSME high pressure fuel duct.

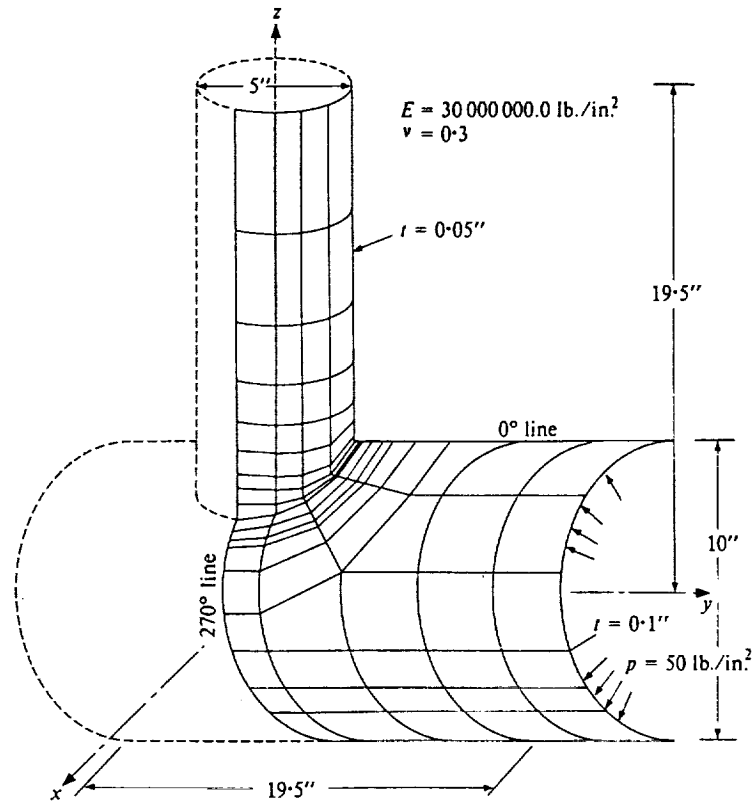
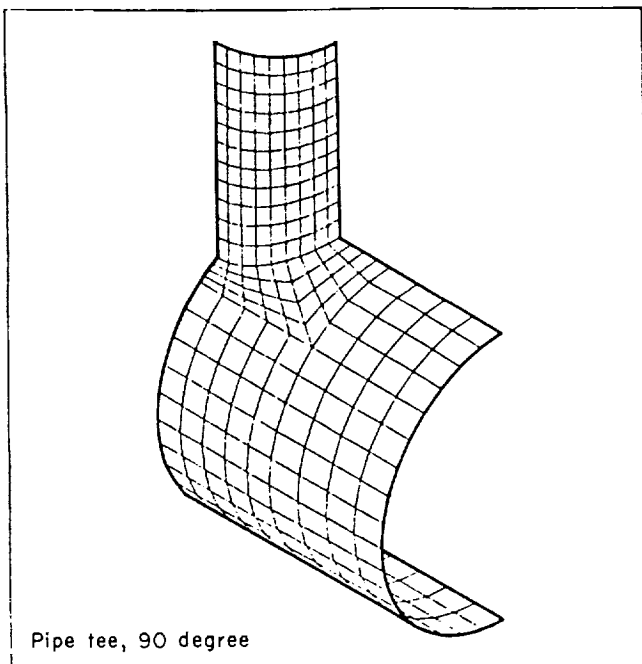
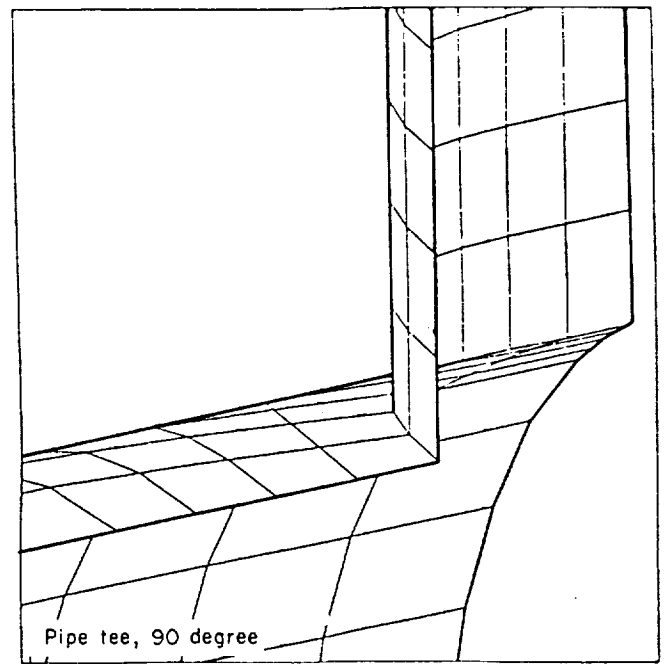


Figure 3. Cylinder-to-cylinder intersection.¹



(a)



(b)

Figure 4. (a) Shell model for a pipe tee, (b) local region of the model.

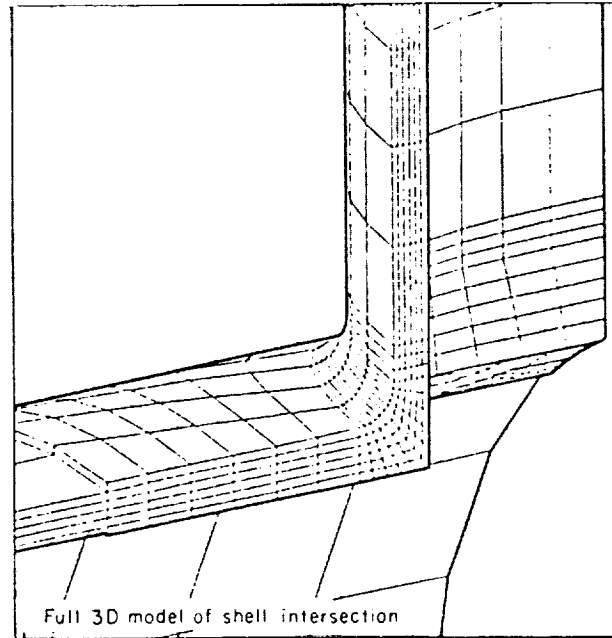


Figure 5. 3-D solid model for a pipe tee.

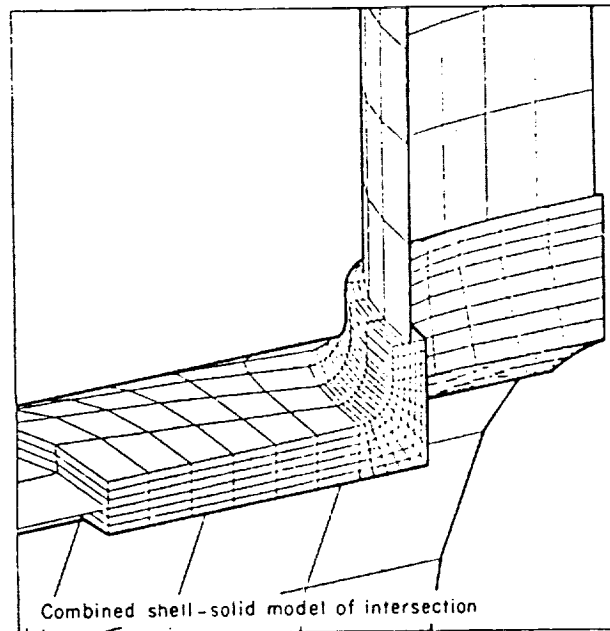


Figure 6. Combined shell and solid model for a pipe tee.

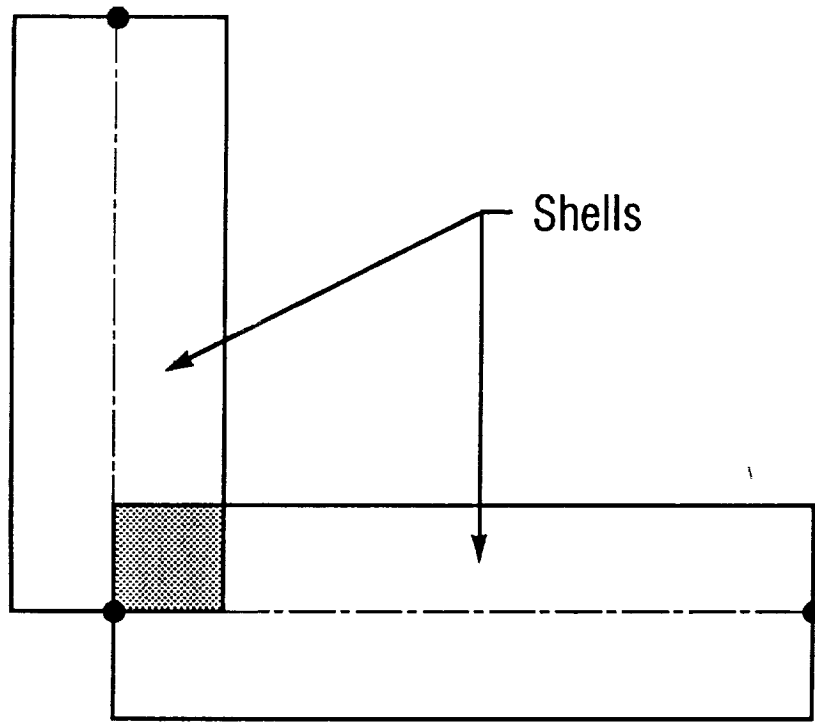


Figure 7. Shell-to-shell intersection.

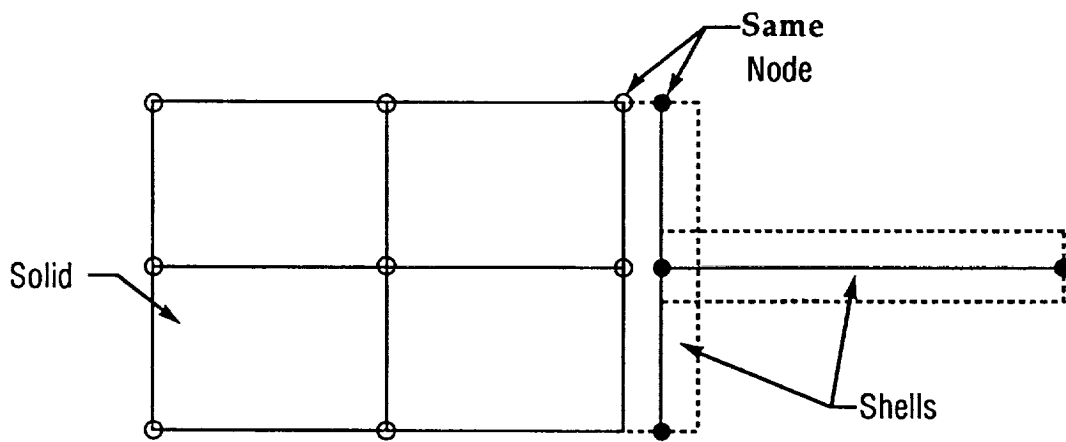


Figure 8. Additional shell elements across the perpendicular free faces of solids.

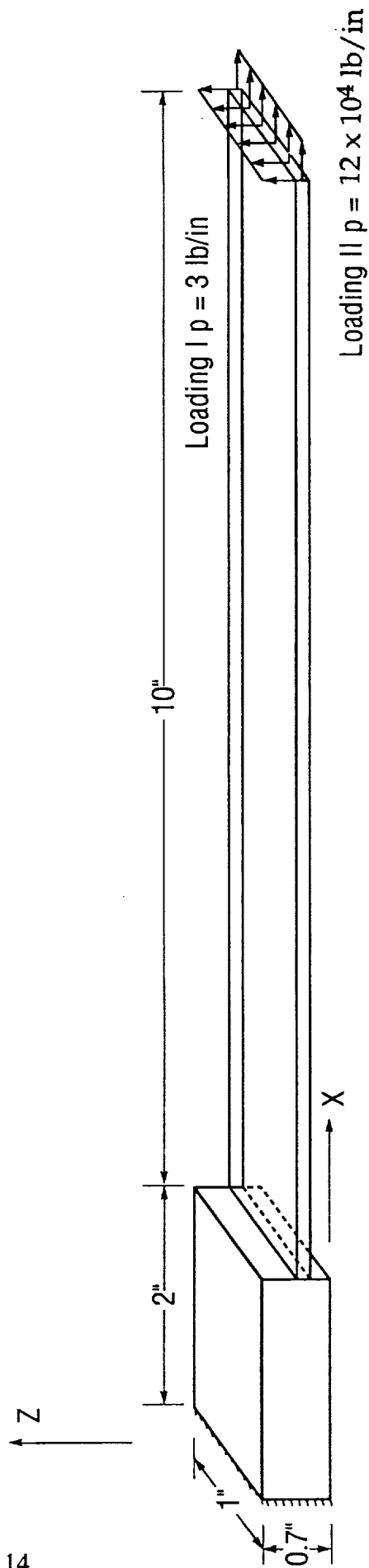


Figure 9. Model used for study (ref. 6).

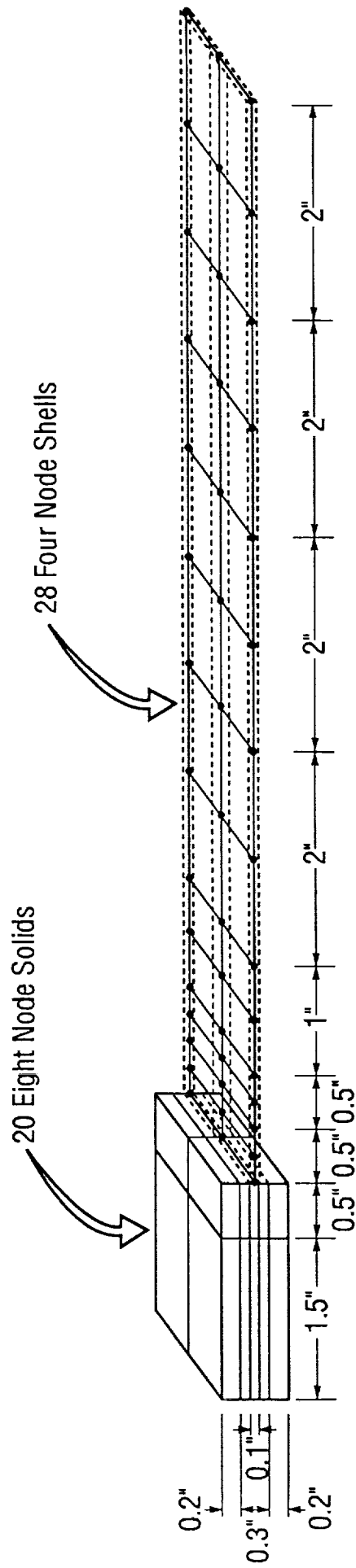


Figure 10. Model A.

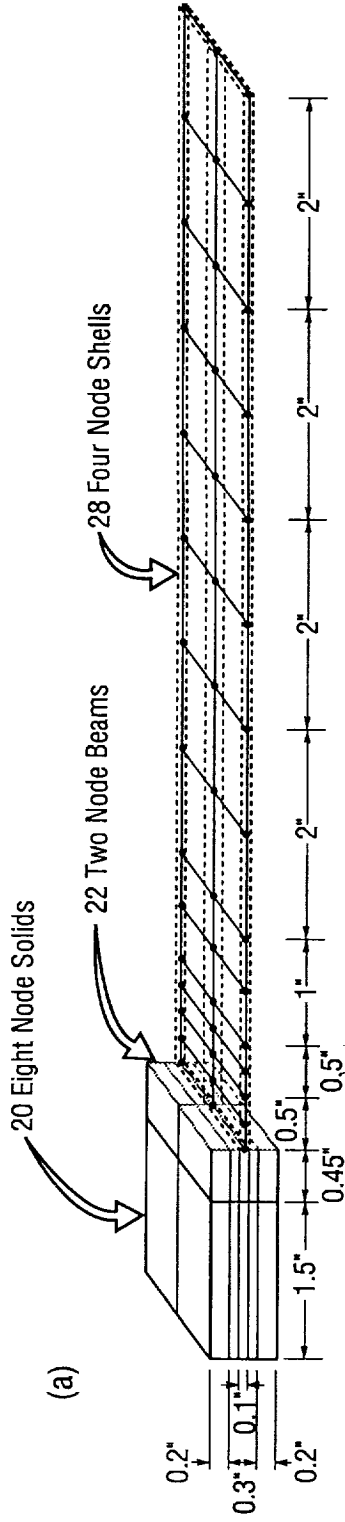


Figure 11. Model B.

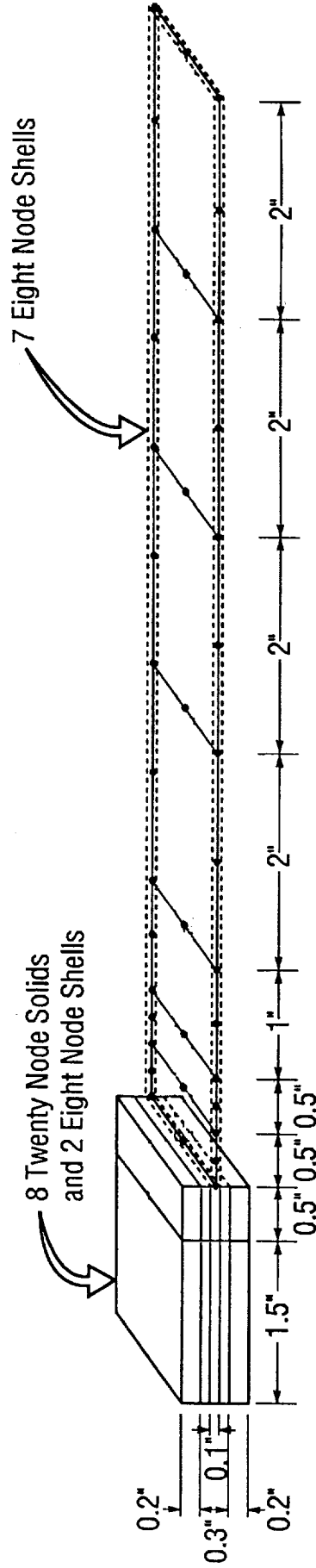


Figure 12. Model C.

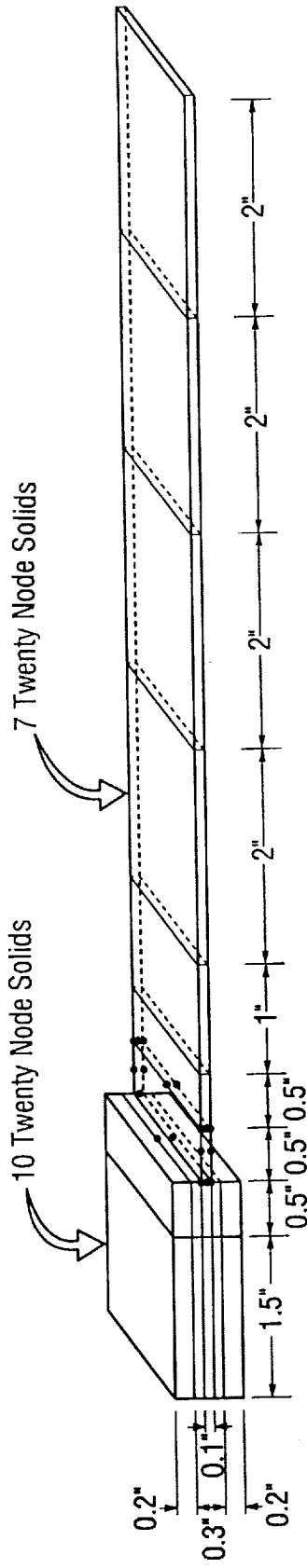


Figure 13. Model D.

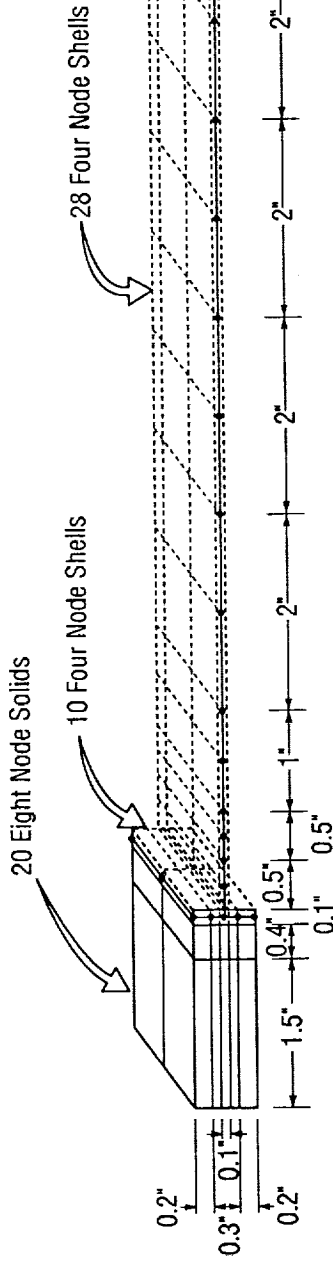


Figure 14. Model E.

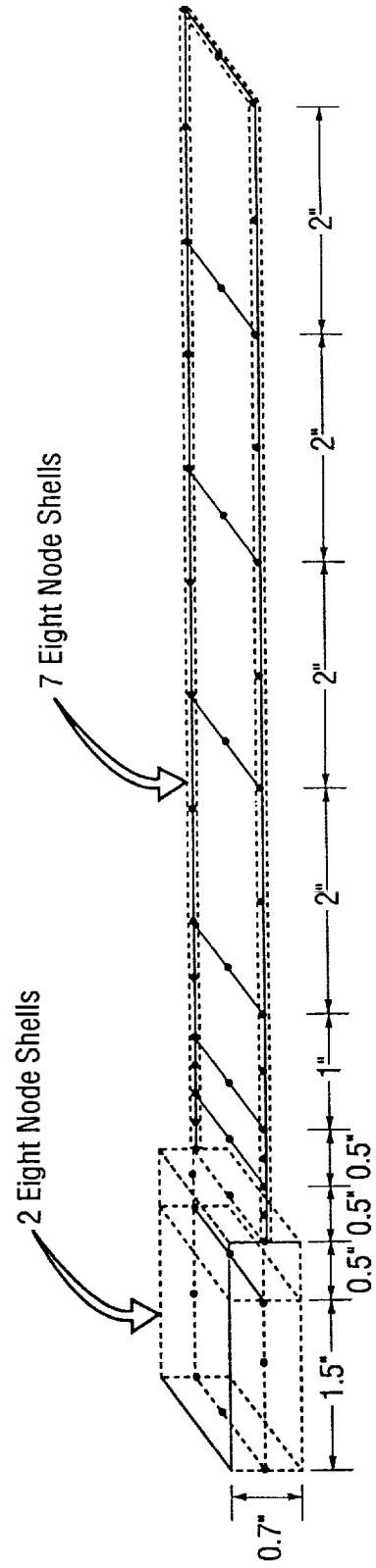


Figure 15. Model F.

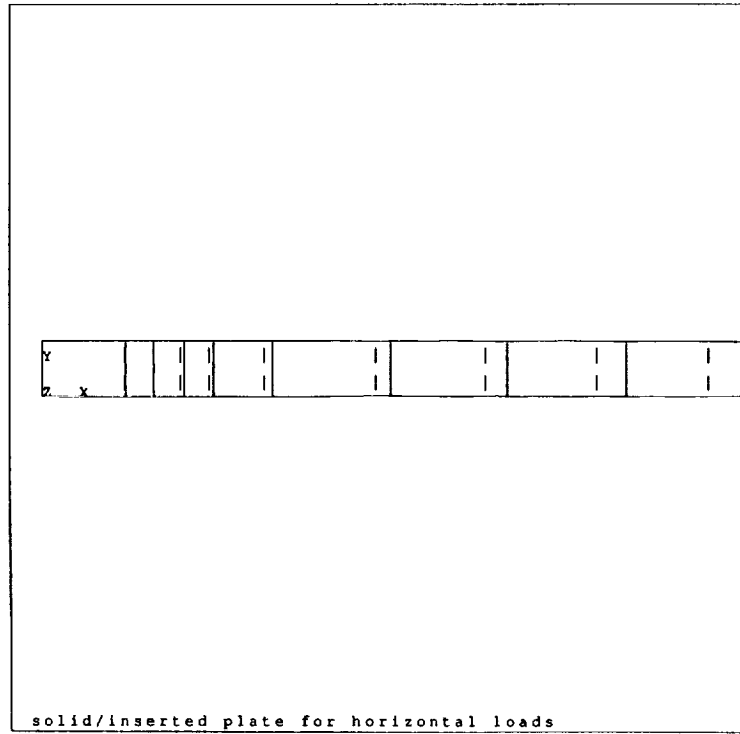


Figure 16. Top view of model C.

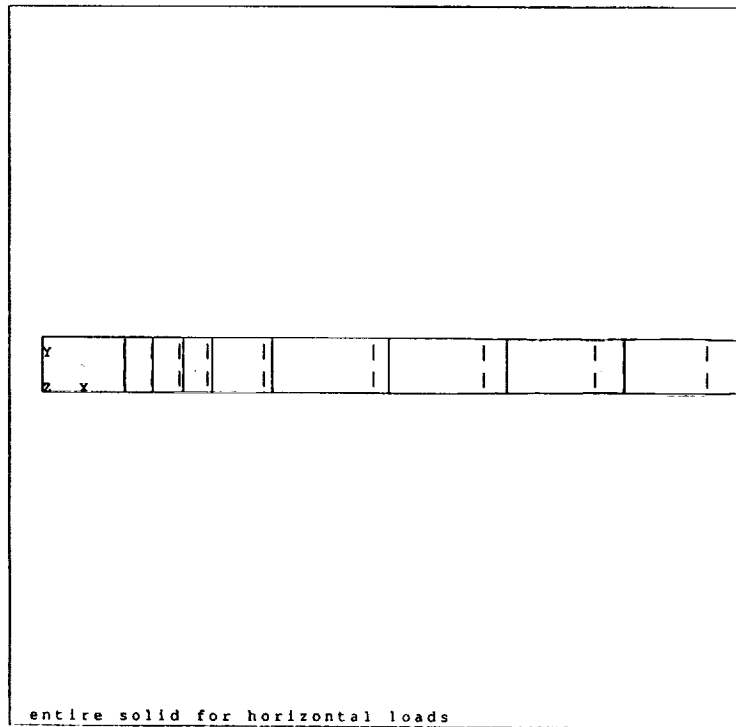


Figure 17. Top view of model D.

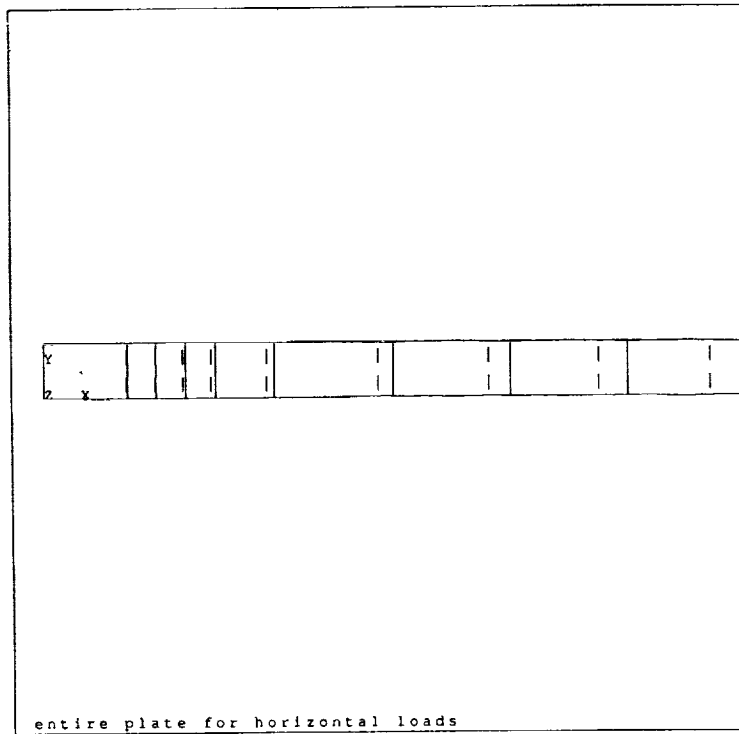


Figure 18. Top view of model F.

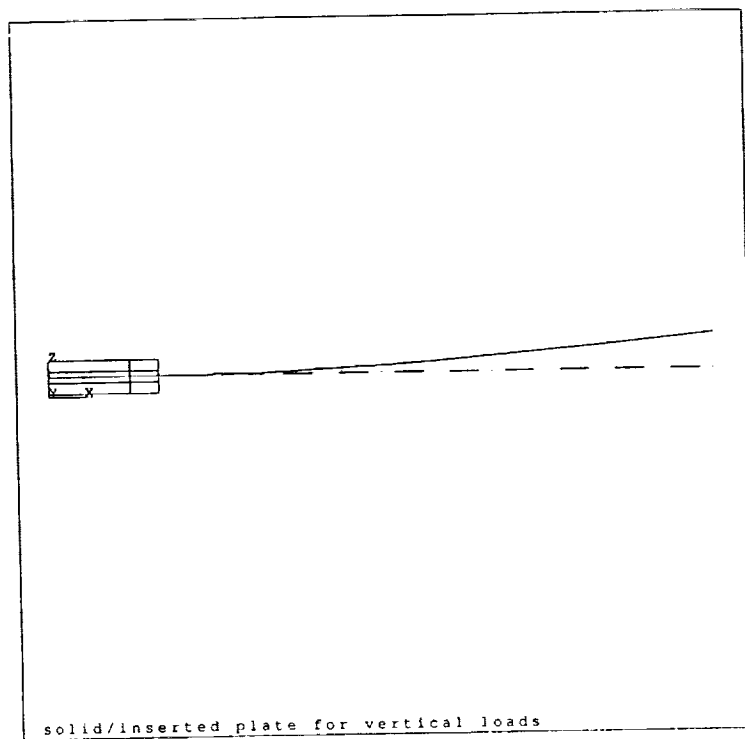


Figure 19. Front view of model C.

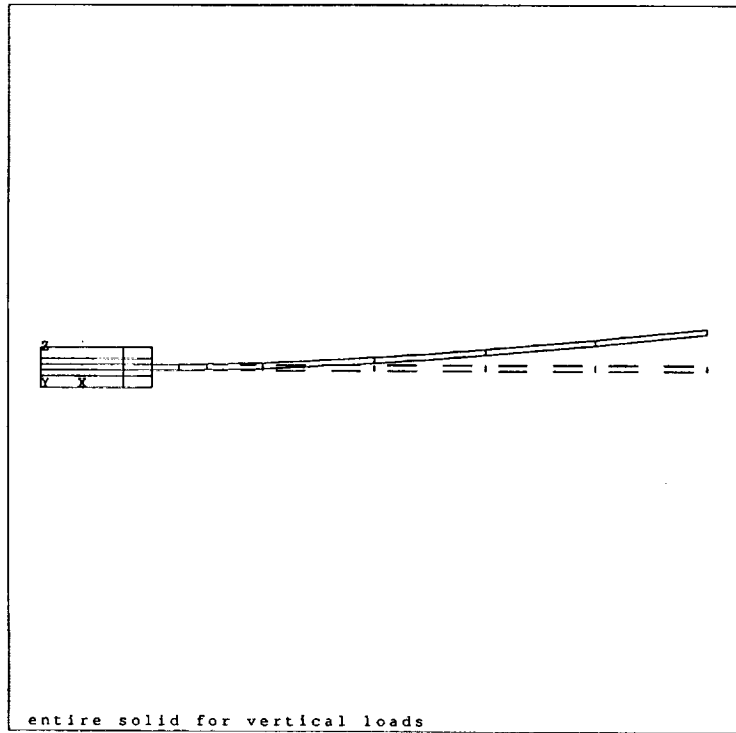


Figure 20. Front view of model D.

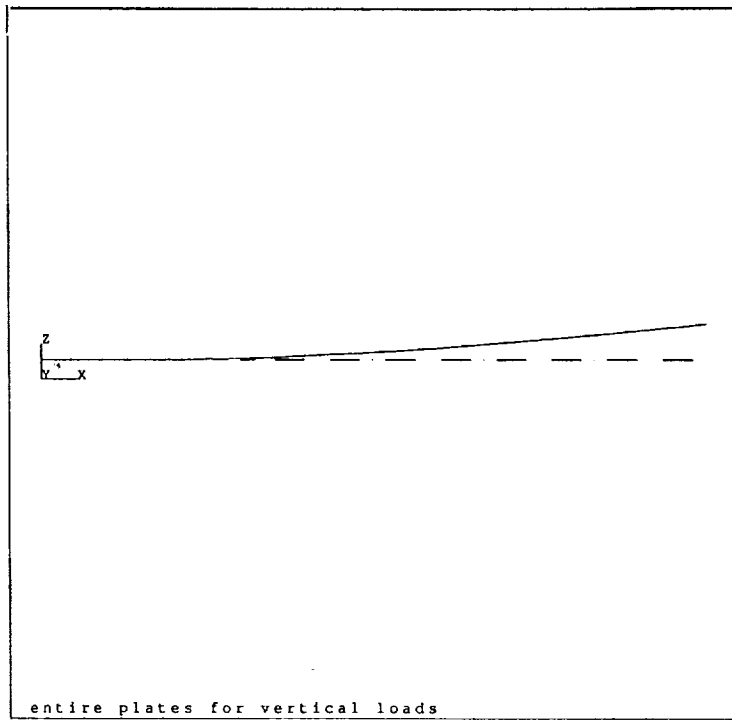


Figure 21. Front view of model F.

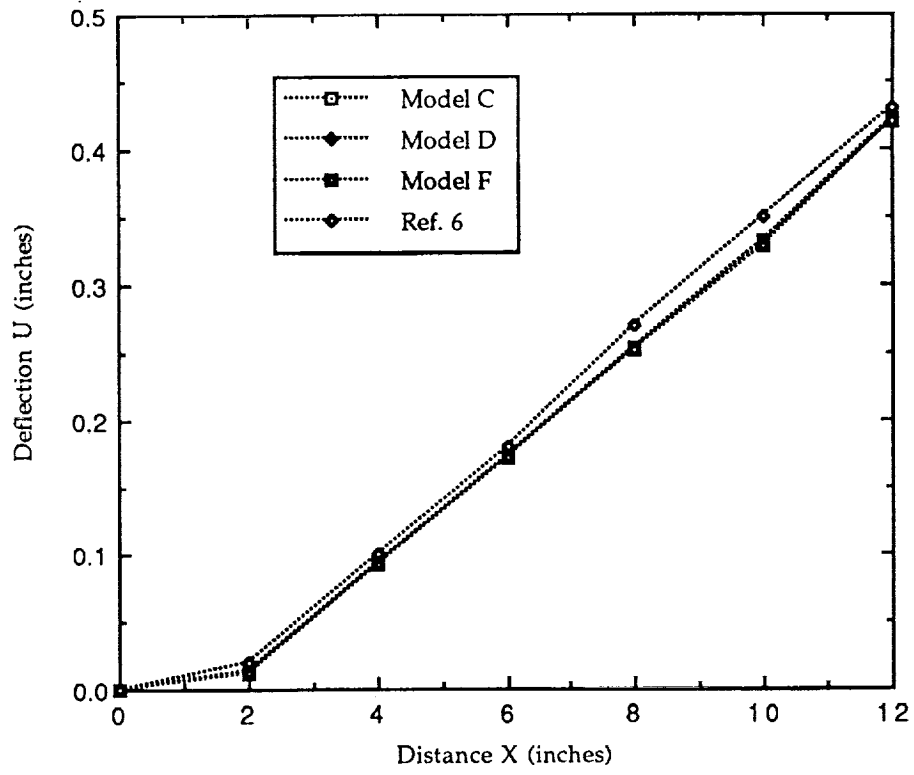


Figure 22. Deflection U along length of model under horizontal load.

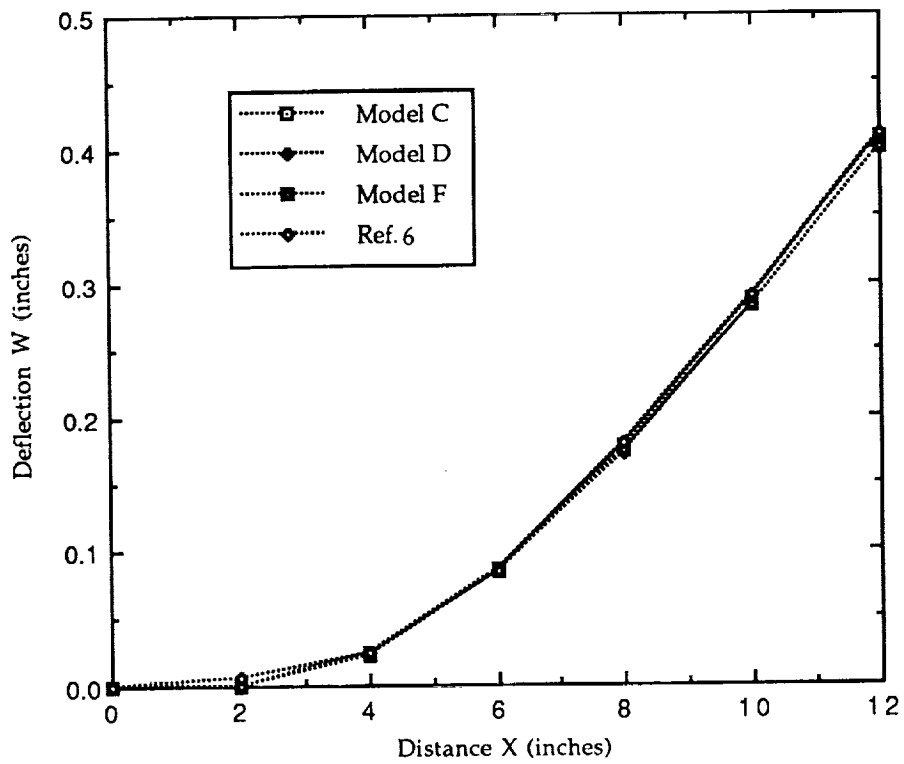


Figure 23. Deflection W along length of model under vertical load.

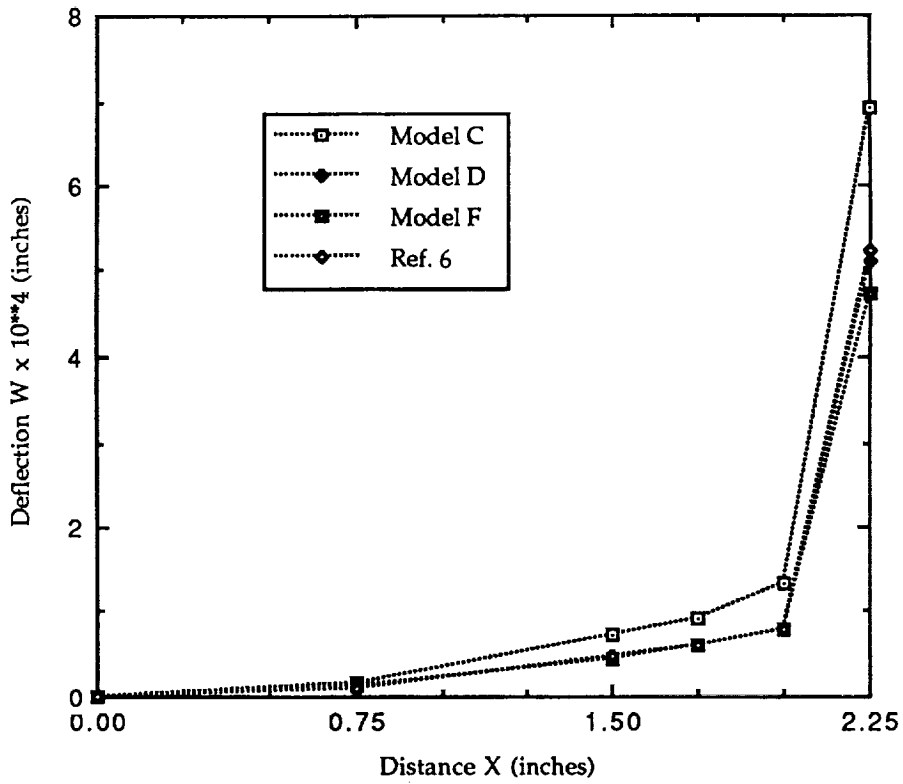


Figure 24. Deflection W along $0 \leq x \leq 2.25$ in under vertical load.

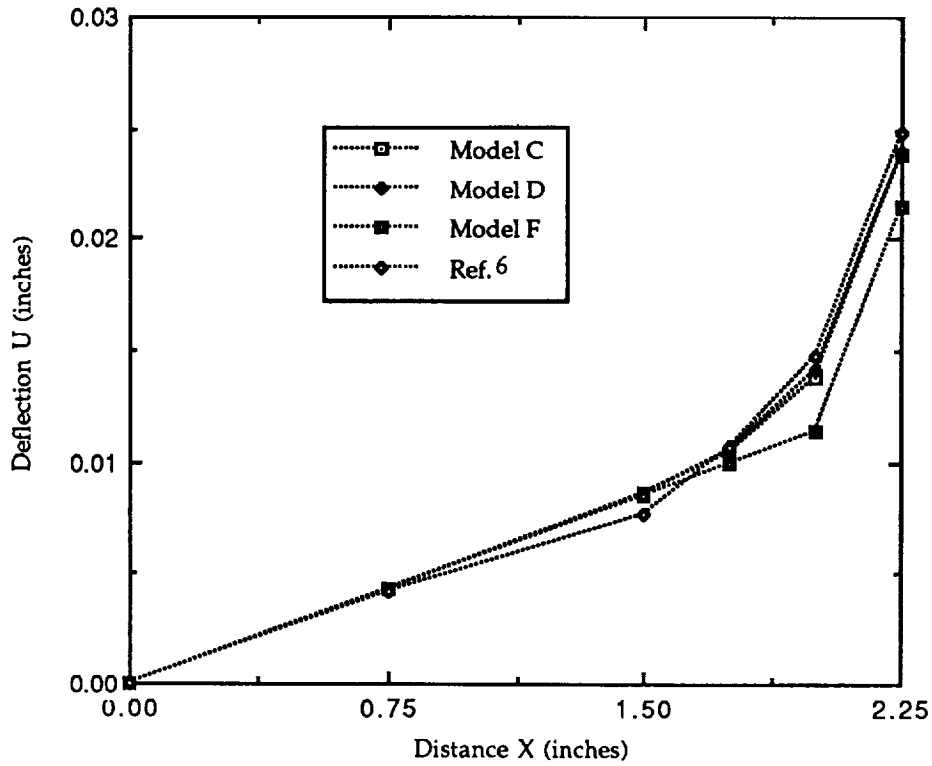


Figure 25. Deflection U along $0 \leq x \leq 2.25$ in under horizontal load.

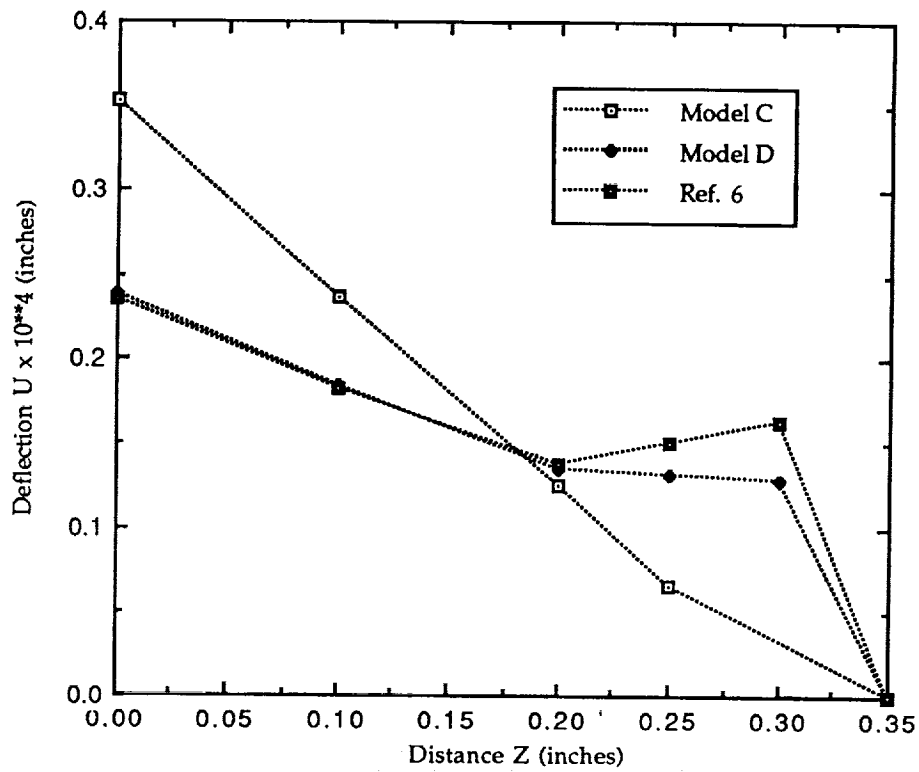


Figure 26. Deflection U along depth of model at $x = 2.0$ in under vertical load.

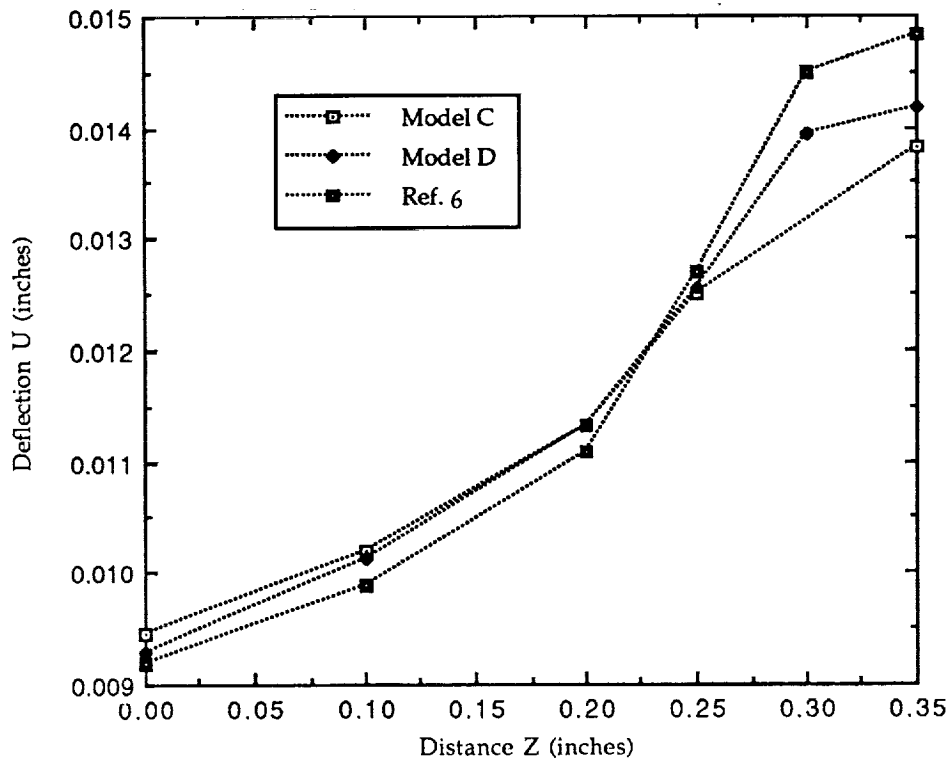


Figure 27. Deflection U along depth of model at $x = 2.0$ in under horizontal load.

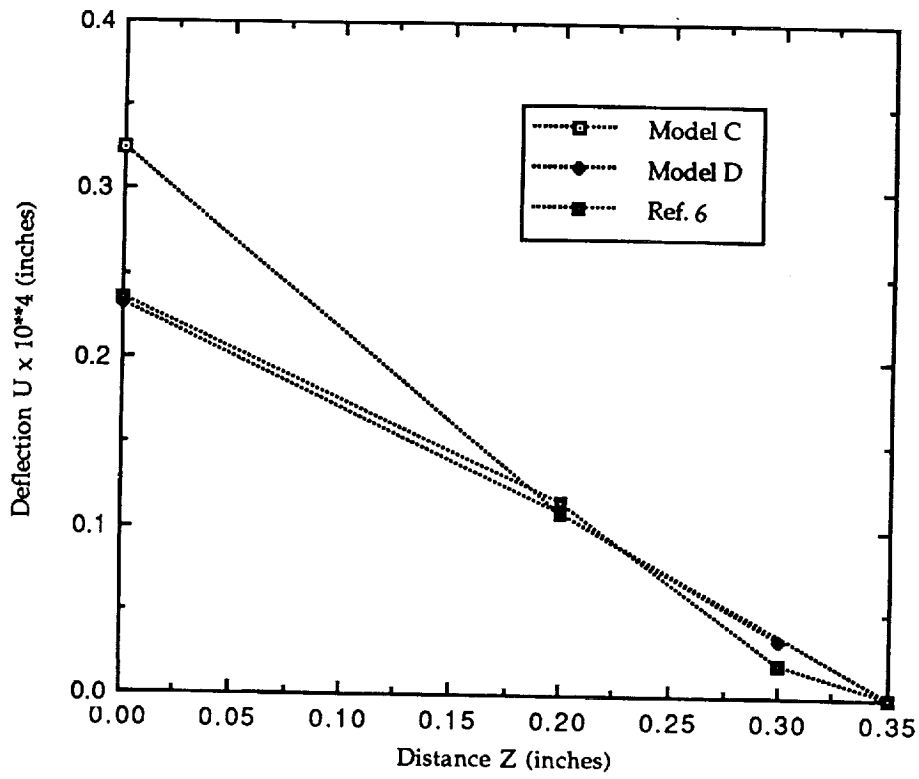


Figure 28. Deflection U along depth of model at $x = 1.75$ in under vertical load.

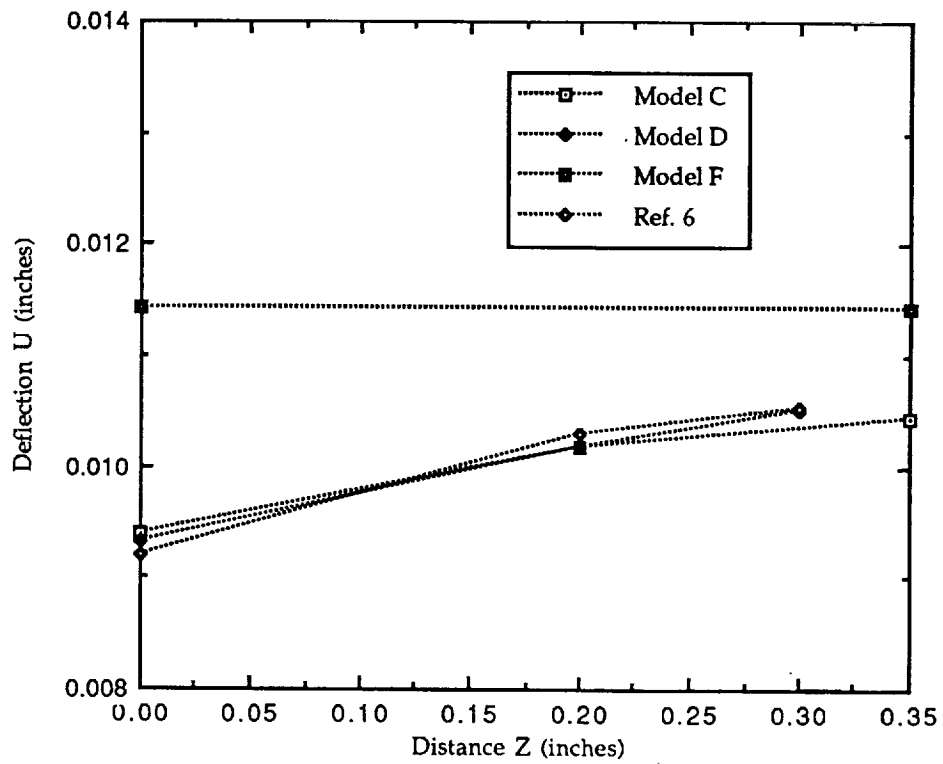


Figure 29. Deflection U along depth of model at $x = 1.75$ in under horizontal load.

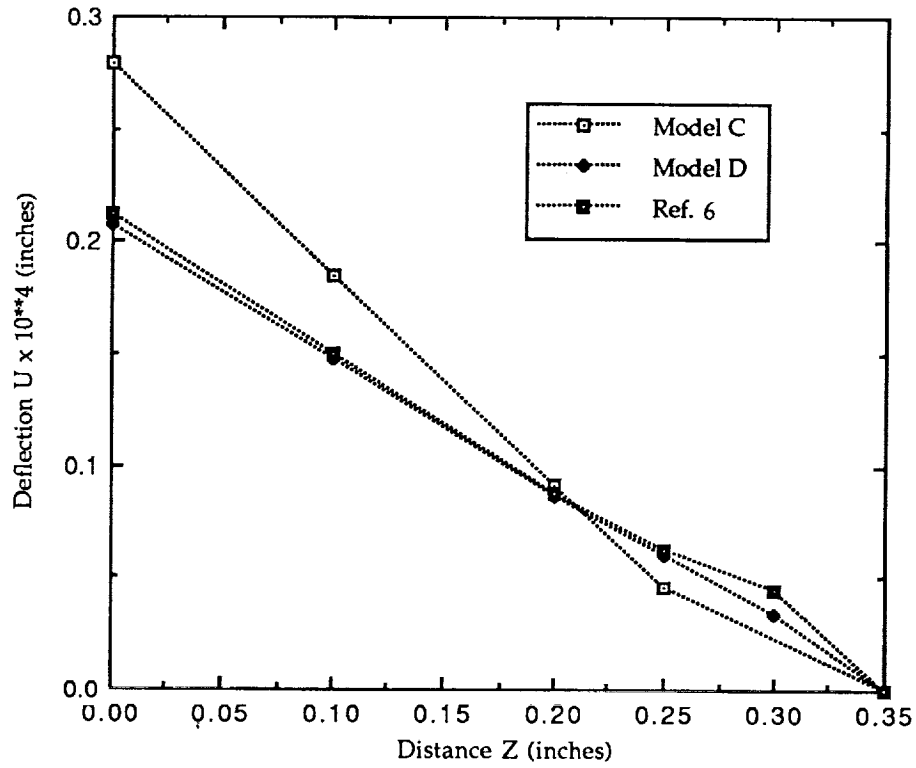


Figure 30. Deflection U along depth of model at $x = 1.5$ in under vertical load.

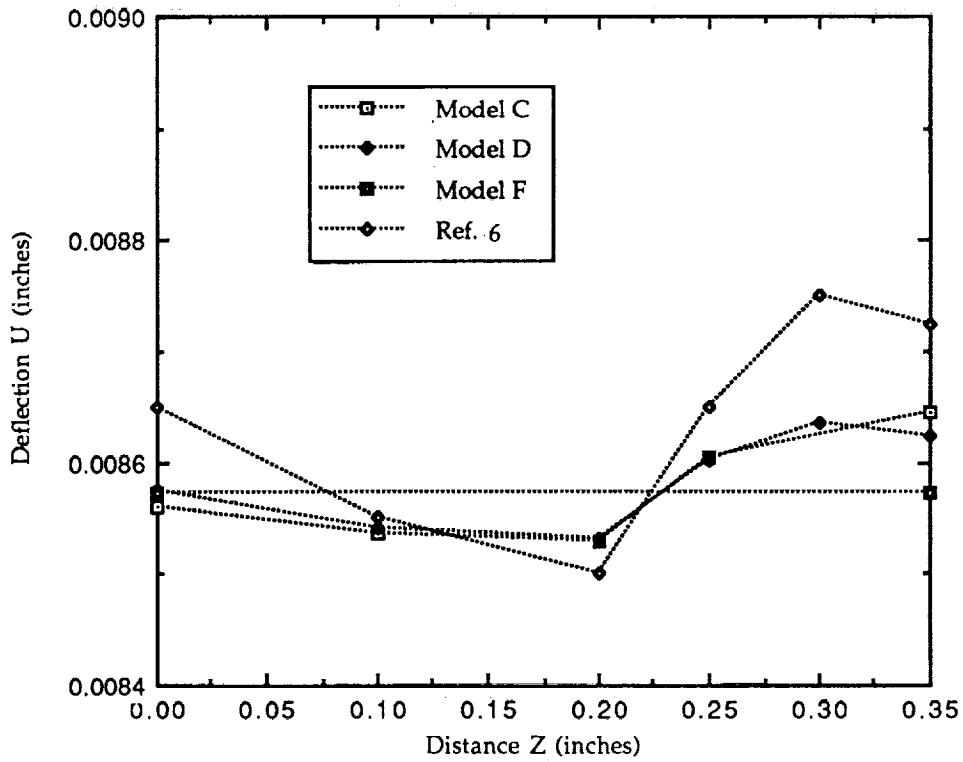


Figure 31. Deflection U along depth of model at $x = 1.5$ in under horizontal load.

APPROVAL

AN ASSESSMENT ON FINITE-ELEMENT MODELING TECHNIQUES FOR THICK-SOLID/THIN-SHELL JOINTS ANALYSIS

By J.B. Min and S.G. Androlake

The information in this report has been reviewed for technical content. Review of any information concerning Department of Defense or nuclear energy activities or programs has been made by the MSFC Security Classification Officer. This report, in its entirety, has been determined to be unclassified.



J.C. BLAIR

Director, Structures and Dynamics Laboratory

